Microchimica Acta (2020) 187: 123
https://doi.org/10.1007/s00604-019-4099-9

ORIGINAL PAPER

CuO/Cu composite nanospheres on a TiO_2 nanotube array for amperometric sensing of glucose

Zhiru Zhou[1] · Zanzan Zhu[1,2] · Feiyun Cui[1] · Jiahui Shao[3] · Hong Susan Zhou[1]

Received: 1 October 2019 / Accepted: 26 December 2019 / Published online: 13 January 2020

Abstract

A non-enzymatic glucose sensor based on the use of CuO-Cu nanospheres placed on a TiO2 nanotube (TNT) array with excellent performance is described. The electrode was fabricated by coating the CuO-Cu nanospheres onto the TNT array through electrochemical deposition. The CuO-Cu nanospheres with a diameter of ~200 nm are well dispersed on the TNT surface, which warrants smooth interaction and a 3D nanostructure with high uniformity. The modified electrode was then used for amperometric determination of glucose in 0.1 M NaOH solution. Figures of merit include (a) a typical working voltage of 0.65 V (vs. Ag/AgCl). (b) a linear range as wide as from 0.2–90 mM, (c) good sensitivity (234 μA mM^{-1} cm^{-2}), and a 19 nM lower detection limit. The sensor is selective over ascorbic acid (AA), dopamine (DA), uric acid (UA), lactose, sucrose, and fructose.

Keywords CuO-Cu nanospheres · TiO_2 nanotube arrays · Amperometric sensing · Wide analytical range · Enzymeless sensing · Glucose sensor

Introduction

Glucose monitoring is important in many clinical and industrial areas [1–4]. Current glucose sensors are mainly composed of two types: enzymatic and non-enzymatic sensors. Enzymatic glucose sensor based on glucose oxidase (GOx) is most widely used in the entire sensor market mainly due to its high selectivity toward glucose and the wide detection range. Current market is dominated by enzymatic glucose sensor but there are many critical drawbacks. All types of enzymatic glucose sensor necessitate enzyme immobilization and it inevitably influenced by the uncertainty of artificially biological substances. Because of the oxygen dependency of enzymatic glucose sensor, oxygen deficiency can cause signal deviation [5]. It also suffers from several drawbacks such as limited durability, high cost, critical operation conditions, complicated electrode construction, and challenges in direct electron transfer [6, 7]. Non-enzymatic glucose sensor emerged as next generation of glucose sensor by using functionalized nanomaterials to directly electro catalyze the glucose oxidation. The choose of the nanostructured and electrocatalytic material is one crucial step for non-enzymatic glucose sensor. Many efforts have been devoted to explore nanostructured material as electrode [7, 8]. For instance, transitional metals (Pd [9], Pt [10, 11], Au [12], Ni [13] and Cu [14]), metal alloys (Pt-Ni [15, 16], Pt-Au [17]), and metal oxide (CuO [18], Cu_2O [19], NiO [13], $NiCo_2O_4$ [20], Fe_3O_4 [21]). Among these materials, copper and its oxide-based nanomaterials showed great electrochemical catalytic properties toward glucose sensing. The composite material of nanostructured copper oxide (CuO and Cu_2O) and Cu was found to promote the redox reactions due to multiple valences and redox couples on the surface oxide layer. As the inherent conductivity of copper oxide is very poor and not favorable for electrode, introducing metallic Cu can facilitate electron transfer of electrode. Thus, catalytic nanoparticles combining both Cu and copper oxide can help promote the electrochemical glucose sensing and increase conductivity. Titania (TiO_2) nanotube arrays are excellent candidates to serve as supporting matrix for loading catalytic metal/metal oxide nanoparticles [22, 23] due to its large specific surface area,

✉ Hong Susan Zhou
szhou@wpi.edu

[1] Department of Chemical engineering, Worcester Polytechnic Institute, Worcester, MA 01609, USA

[2] National Cancer Centre Singapore, 31A Nanyang Ave. #07-02, Singapore 639804, Singapore

[3] School of Environmental Science and Engineering, Shanghai Jiao Tong University, 800 Dongchuan Road, Shanghai 200240, China

excellent thermal stability and biocompatibility. Its vertically aligned nanostructures not only facilitate catalysts absorbed onto the surface of TiO_2 nanotubes but also promote rate of electron transfer. Other than the selection of material, the morphology of assembled nanomaterials in terms of shape and size is another contributing factor. It was found that [24] an electrode consisting of homogeneous particle contributed to electrochemical properties by forming a regular network. Well-ordered nanostructured anode materials can reduce the diffusion length of Li^+ and improve the cycling performance for lithium-ion battery [25].

Current non-enzymatic glucose sensors show major drawbacks of linear range outside physiological range and poor selectivity to glucose in presence of other sugars. We successfully fabricated CuO-Cu/TiO_2 electrode by depositing the CuO-Cu nanospheres onto TiO_2 nanotube arrays surface through electrochemical deposition method, which is a fast procedure. The CuO-Cu modified electrode were then used as the working electrode, while Ag/AgCl as reference electrode and Pt wire as counter electrode. The electrochemical properties of the electrode toward glucose oxidation were studied under alkaline condition in 0.1 M NaOH solution. The sensor exhibited a wide linear range between 0.2–90 mM with high sensitivity of 234 μA mM^{-1} cm^{-2} toward glucose sensing. This wide linear range is very promising in real application as blood glucose concentrations are typically in the range of 4.9–6.9 mM for healthy patients, increasing to up to 40 mM in diabetics after glucose intake; Moreover, glucose concentration can increase up to 80 mM for biopharmaceutical industry [26]. In light of this information, the proposed non-enzymatic glucose sensor has great potential for continuous monitoring of glucose in most clinical and biopharmaceutical applications.

Experimental session

Chemicals and reagents

Titanium foil (0.25 mm, 99.7% trace metals basis), ammonium fluoride (NH_4F), ethylene glycol (99.8%), copper sulfate (≥99.9 %), D-(+)-glucose (≥99.5 %), ascorbic acid (AA), dopamine (DA), uric acid (UA), D-lactose, sucrose, and fructose were all purchased from Sigma Aldrich (https://www.sigmaaldrich.com/technical-service-home/product-catalog.html).

Preparation of the TiO_2 nanotube array (TNT)

A sheet of titanium (99.7% trace metals basis, Aldrich) was cut into several small foils with the size of 2.5 cm by 2 cm. Then the foils were polished manually with sandpaper (220–400-800 assorted grit, 3 M Wetordry) for 30 min and cleaned sequentially with methanol, acetone, ethanol, and deionized water (DI water) using an ultrasonic cleaner for 15 min each. After that, 5 mL of DI water, 15 mL of 70% HNO_3 acid, and 5 mL of 50% HF acid was mixed to make 25 mL of HF/HNO_3 mixed acid (1:3:1 ratio in volume). The cleaned titanium foils were then immersed into the mixed acid for 15 s and rinsed by DI water.

3.351 g of NH_4F solid was dissolved in 270 mL of ethylene glycol and 30 mL of DI water (1 wt% NH_4F in ethylene glycol electrolyte containing 10 vol% of water) to make the electrolyte solution for anodization. A piece of cleaned Ti foil and a platinum mesh (1.5 cm × 2 cm) were carefully immersed in parallel into the electrolyte to form a two electrodes electrochemical cell and connected to a direct current (DC) power supply station (DCS80-13E, Sorensen). Ti foil was anodized under different pairs of voltages and times under stirring (reaction area: 1.5 cm × 1.5 cm). The attempted voltage range was between 20 V and 30 V, and anodizing time varied from 20 to 100 min. The anodized foils were rinsed with DI water. Finally, the final foils were annealed at 350 °C for 1.5 h and then cooled naturally to room temperature.

Preparation of CuO-Cu/TNT electrode (CuO-Cu/TNT)

CuO-Cu NPs were deposited onto the TiO_2 nanotube array electrode through a two-step electrodeposition method [17]. A constant potential of −0.37 V was first applied to the TiO_2 nanotube in a solution of 50 mM $CuSO_4$ + 0.5 M H_2SO_4 for 100 s to deposit Cu first. Then, the electrode was scanned in 0.1 M NaOH with cyclic voltammetry (CV) under the potential range of −0.5 to 0.3 V at 100 mV s^{-1} for 10 cycles to allow the partly oxidization of Cu to CuO nanospheres.

Characterization

Scanning electron microscopy (SEM, JEOL, JSM-7000F) operating at 10 kV was applied to characterize the morphology of samples. Structural analysis of the TiO_2 nanotube arrays and CuO-Cu /TiO_2 nanotube arrays was investigated by X–ray diffraction (XRD, Bruker-AXS D8 focus, 40 kV, 40 mM, Cu Ka radiation). All electrochemical measurements were carried out using an Autolab PGSTAT12 electrochemical workstation (Metrohm, USA Inc.). A conventional cell with a three-electrode configuration were used throughout this work. The working electrode is the TiO_2 nanotube array. A platinum mesh and an Ag/AgCl (saturated KCl) were used as the counter electrode and the reference electrode, respectively. All the electrolytes were deaerated by bubbling nitrogen gas for 30 min before the experimental procedure. All the experiments were carried out at room temperature.

Results and discussion

Characterization of CuO-Cu/TNT

The structural and morphological information were carefully studied by XRD and SEM. Figure 1a and b shows the XRD patterns of TiO_2 nanotube arrays and CuO-Cu nanospheres deposited TiO_2 nanotubes respectively. The observed diffraction peaks can be assigned to Cu, CuO, anatase TiO_2 and Ti substrate. The diffraction peak at 25.4° can be easily indexed to the (1 0 1) plane of TiO_2 anatase phase (JCPDS card NO.21–1272), while peaks at 40.3°, 53.1°,63.0°, 70.8° and 76.4° can be attributed to Ti substrate. After electrodeposition, Peaks density at 2θ = 35.5°, 38.4° is much higher, which is corresponded to CuO crystallites (JCPDS card no.65–2309 and JCPDS card NO.44–0706). Aside from that, peaks at 2θ = 43.5°, 50.5° attributed to the (111) (200) planes of Cu with cubic phase (JCPDS card NO.04–0836). Thus, the presence of CuO-Cu was confirmed in the sample after deposition. The morphology of bare TiO_2 nanotube arrays and CuO-Cu/TNT are characterized by SEM and displayed in Fig. 1c and d. TiO_2 nanotubes with a diameter of ~100 nm formed a smooth supporting substrate surface. After the electrodeposition, CuO-Cu nanospheres with a diameter ~200 nm was well dispersed on TNT surface, forming a 3D nanostructure with high uniformity. The intimate interface between the highly electrocatalytic material (CuO-Cu) and conductive supporting substrate TiO_2 nanotubes array (TNT) for electron transfer reactions in the electrode, thus increasing current signal in the electrode. The uniform 3D nanostructure may lower the adsorption of the intermediates after oxidation, which possibly leads to a larger detection range.

Electrochemical oxidation of glucose on CuO-Cu/TNT electrode

The electrochemical properties of Bare TNT and CuO-Cu/TNT electrode was examined by cyclic voltammetry (CV) in 0.1 M NaOH at a scan rate of 100 mV s^{-1}. It was performed in the potential range of 0 to 0.8 V. Because of the direct oxidation of glucose in the alkaline medium [27], NaOH concentration at 0.1 M was reported as the optimal concentration [19]. Figure 2a shows the CV of bare TiO_2 nanotube arrays and CuO-Cu/TiO_2 in absence and presence of glucose. TiO_2 nanotubes as supporting matrix showed no electrocatalytic activity toward glucose as there is no reduction and oxidation peak observed (Line a and b). After modifying the TNT with CuO-Cu nanospheres, only reduction peak appeared in blank NaOH solution (line c) while oxidation peak appeared after the addition of glucose (line d). The reduction peak at about +0.55 V in NaOH correlates with the redox couple Cu (II)/Cu (III): $CuO + OH^- \rightarrow CuOOH^-$, which was reported by previous researchers [28]. After addition of glucose solution, a single oxidation peak occurred corresponding to the glucose oxidation process. The oxidation process starts at approximately +0.2 V with broad peak around +0.45 V. This may be attributed to electro-oxidation of glucose to gluconolactone catalyzed by thermodynamically unstable Cu (III) species according to previous reports [29–31].

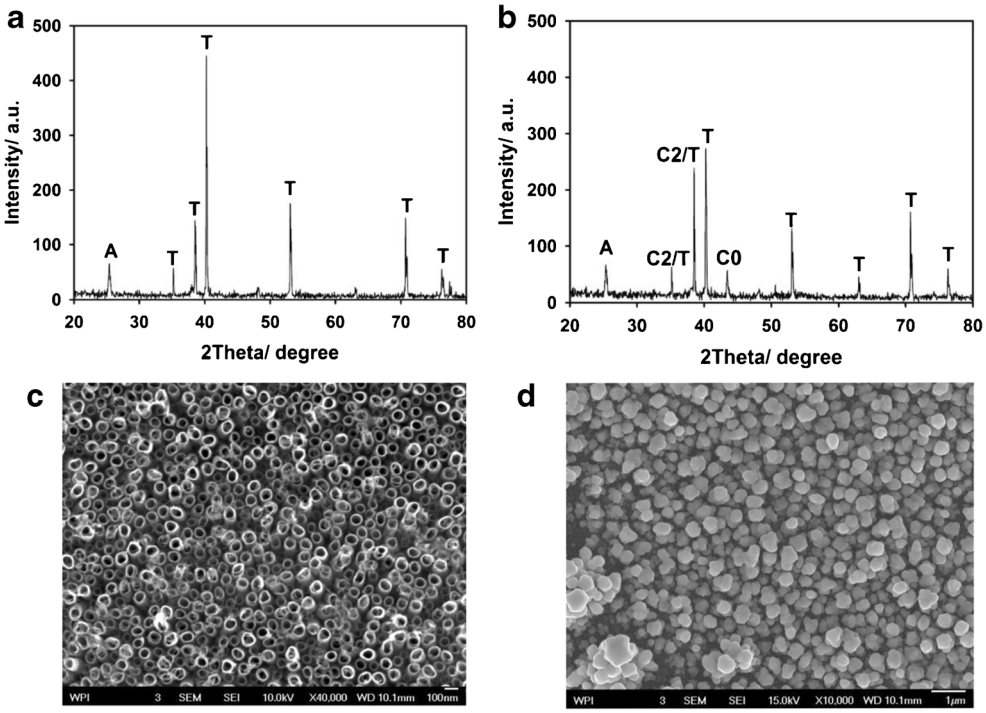

Fig. 1 XRD patterns of (**a**) TiO_2 (**b**) CuO-Cu/TiO2. SEM images of (**c**) TiO_2 nanotubes (**d**) CuO-Cu nanospheres decorated TiO_2 nanotubes

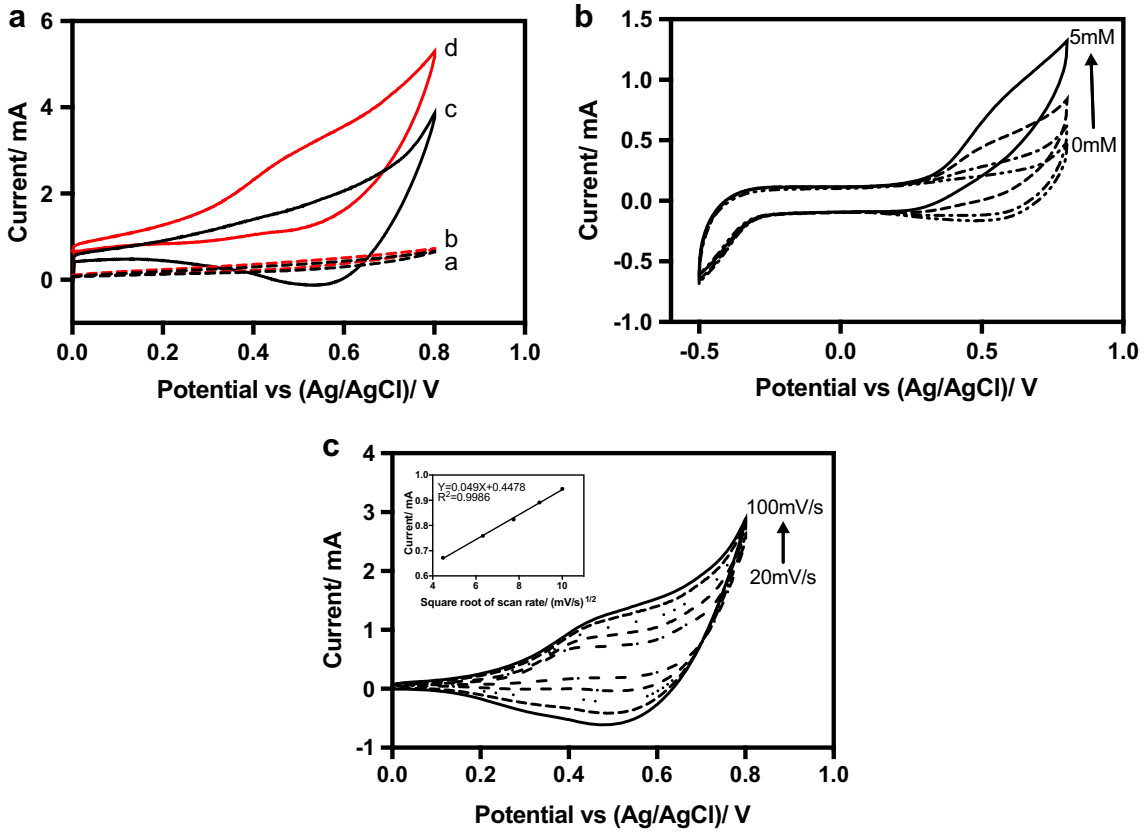

Fig. 2 **a** CVs of bare TiO_2 nanotubes in absence(a)/presence(b) of glucose. CVs of CuO-Cu/TiO_2 in absence(c)/presence(d) of glucose. **b** CVs of CuO-Cu/TiO_2 in presence of different concentration of glucose between potential range of −0.5-0.8 V (**c**) CVs of CuO-Cu/TiO_2 electrode obtained in 0.10 M NaOH solution containing 2 mM glucose at different scan rates (inner to outer): 20, 40, 60, 80, 100 mV/s. And the dependence of the oxidation peak current density of glucose on scan rate (left inlet)

To fully understand the glucose electro-oxidation process, CV responses of CuO-Cu/TNT electrode with different concentration of glucose (0, 0.5, 2, 5 mM) are shown in Figure 2b. The oxidation peak starts with an onset of +0.2 V which is corresponded to glucose electrooxidation process. As expected, the anodic peak currents gradually increase with increasing of glucose concentration from 0 to 5 mM. The result is in accordance with the Randles-Sevcik equation, $i_p = 268600n^{\frac{3}{2}}AD^{\frac{1}{2}}C\upsilon^{\frac{1}{2}}$, where i_p is the peak current, A as electrode surface area, D as diffusion coefficient, C as the concentration, and υ as the scan rate. We also noticed a gradual positive shift of oxidation peak with increasing concentration of glucose, it may be attributed to the interaction of glucose with the electrode surface covered with low valence copper species. As it is reported by Wang [32] that the glucose oxidation occurred with wide peak around +0.60 V on Cu foil electrode and it will negatively shift to +0.48 V at the CuO nanoplatelets electrode. This confirmed that Cu is also responsible for the glucose oxidation, and the process is reported [33] as multi-steps including the formation of strong oxidizing Cu (III) species. Thus, for our CuO-Cu/TNT electrode, CuO species are initially reduced to form Cu (III). When the glucose is at high concentration, the Cu species get to be involved in the electrooxidation, generating wider detection range. The combination of Cu and CuO not only increase conductivity but also facilitate electrochemical properties.

Figure 2c shows the effect of scan rate (20–100*mV/s*) of CuO-Cu/TNT in 0.1 M NaOH solution in the presence of 2 mM glucose. It was found that the current peaks of glucose oxidation increases linearly with square root of scan rate (Left inlet) in accordance with the Randles-Sevcik equation, indicating a surface-controlled electrochemical process [34].

Amperometric response of the electrode

To test the analytical performance of glucose sensor, amperometric measurements were performed in 0.1 M NaOH solution with magnetic stirring. A linear relationship can be drawn between current and glucose concentration within the detection range. While applying high potential is useful for getting a wide linear range [35], a high potential may lead to large interference signals resulting non-specificity. In our experiment, an optimized potential of +0.65 V was obtained taking

consideration of these two factors. Figure 3a shows the amperometric response under +0.65 V with step-wise addition of glucose solution (0.2–8 mM) with an interval time of 30 s. The linear relationship between current and concentration is settled in a wide range of 0.2–90.4 mM, which is much superior to other non-enzymatic glucose sensor. Figure 3b shows the corresponding calibration plot (current response versus glucose concentration), which exhibited a linear dependence on glucose concentration ($I = 0.0117C + 0.1391$, $R^2 = 0.9996$). From linear regression equation, the sensitivity(S) of CuO-Cu/TiO_2 is calculated as 234 μA mM^{-1} cm^{-2} by dividing the slope of linear calibration plot with electrode surface area. Limit of detection is calculated as 0.019 μM according to $LOD = 3\ S_b/S$, where 3 is the noise to signal ratio (S/N), S_b is the standard deviation of blank solution, and S is the sensitivity. The good sensitivity and low LOD may be attributed to three significant factors: (i) multi redox couples of CuO/Cu composite nanospheres improve the electrocatalytic properties (ii) the presence of Cu provides good conductivity to the CuO-Cu/TiO_2 electrode. (iii) High uniformity of nanostructure facilitates the mass transport of glucose onto the electrode.

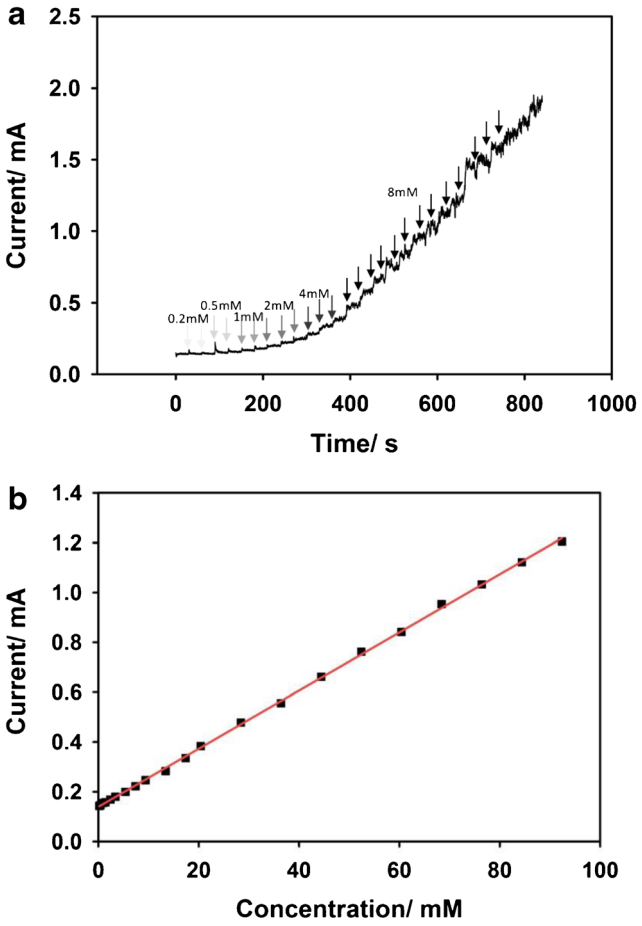

Fig. 3 **a** Amperometric measurement of CuO-Cu/TiO_2 electrode responses to stepwise addition of glucose (0.2 mM–8 mM) in 0.10 M NaOH solution at potential at 0.65 V. **b** The calibration plot of the current response versus glucose concentration

The stability of the current response was investigated by current response to 4 mM glucose during a long operational period of 30 min (Fig. 4). The CuO-Cu/TiO_2 response to one time adding of glucose solution was stable with a loss of only 3.5% in current signal, indicating high reliability of the response signal.

Selectivity and short-term stability

Selectivity is another important performance parameter for a biosensor, especially in practical applications. The selectivity of CuO-Cu/TiO_2 was tested with various interference species. Ascorbic acid (AA), Uric acid (UA) and dopamine (DA) are representative electroactive interferences coexisting with glucose in blood. The normal physiological level of glucose in human blood is 3–8 mM compared to about 0.1 mM of interfering species (with Glucose/interferents ratio of more than 30:1) [36], however the Glucose/interferents ratio is much lower in food samples and biopharmaceutical industry (with glucose/interferents ratio of 10:1). In food industry and biopharmaceutical industry, there are many other sugars commonly coexisting with glucose as well. Therefore, the interference experiments were carried out by successive injection of 4.0 mM glucose, 0.4 mM Ascorbic acid (AA), Dopamine (DA), Uric acid (UA), Lactose, Sucrose, and Fructose. According to amperometry results (Fig. 5), there was a vivid response of glucose while insignificant responses to interfering species. And the current response to glucose maintained consistent even after adding all the interference species. Thus, it confirms the suitability of CuO-Cu/TiO_2 electrode for the selective detection of glucose in presence of other easy oxidative species and sugars possibly included in blood or bioreactor. The high selectivity makes it a good candidate for both clinical application and biopharmaceutical application.

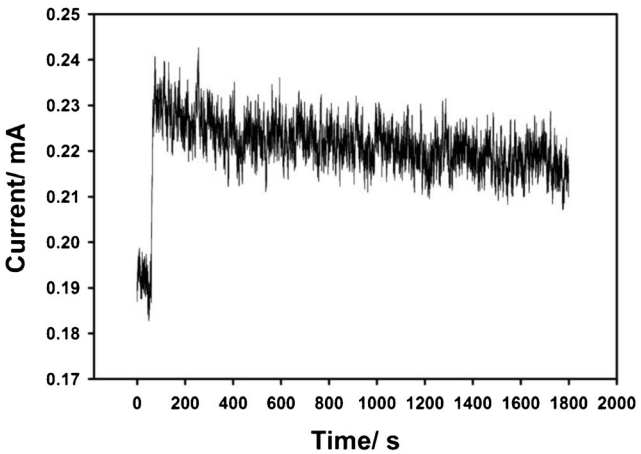

Fig. 4 Amperometric response of sensor over a long operational time of 1800 s

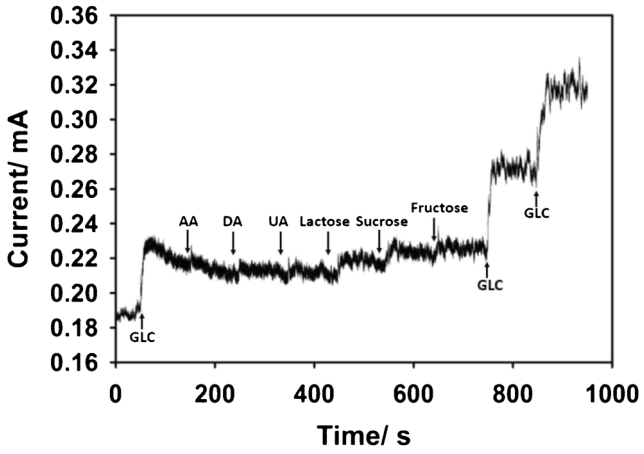

Fig. 5 Amperometric measurement of the CuO-Cu/TiO_2 electrode responses to successive addition of 4 mM glucose, 0.4 mM Ascorbic acid (AA), 0.4 mM Dopamine (DA), 0.4 mM Uric acid (UA), 0.4 mM Lactose, 0.4 mM Sucrose and 0.4 mM Fructose in 0.10 M NaOH solution at 0.65 V

Reproducibility, reusability, and long-term stability

Furthermore, reproducibility, repeatability, and long-term stability are also vital paramaters for non-enzymatic glucose sensor. To evaluate the electrode-to-electrode reproducibility, five electrode were under same conditions, as shown in Fig. 6a, a good relative standard deviation of 4.1% was achieved. The repeatability of CuO-Cu/TNT electrode was also measured with one electrode to detect 4 mM glucose five times and a relative standard deviation (RSD) of 2.12% was obtained. (Figure 6b). The long-term stability of the sensor was investigated by measuring its sensitivity(S)/initial sensitivity(S_0) over successivively five days, about 87% of its initial sensitivity was obtained with the fabricated electrode at the fifth determination (Fig. 6c). The good reproducibility, repeatability and long-term stability makes CuO-Cu/TNT applicable for practical use.

Conclusions

A non-enzymatic glucose sensor was developed by fabricating well-alligned TiO_2 nanotubes with well dispersed CuO-Cu nanospheres on it. The hierarchical 3D structure of nanotubes and nanospheres with high uniformity facilitates electron transfer for electrochemical process. Well dispersed CuO-Cu nanospheres onto substrate generates a smooth electrode surface. This facilitate analyte glucose solution diffusion into electrocatalytic catalyst. Overall, the electrochemical performance of this electrode exhibited wide linear detection range up to 90 mM with high sensitivity and low limit of detection. Good selectivity, stability, and reproducibility. Those excellent sensing performance originate from (a) improved eletrochemical properties because of the presence of nanohybrid CuO/Cu, which possess the synergistic effect between Cu and CuO; (b) high uniformity of nanostructures which simultaneously minimizes the electron transfer resistance for elctrode and diffusion resistance between electrode

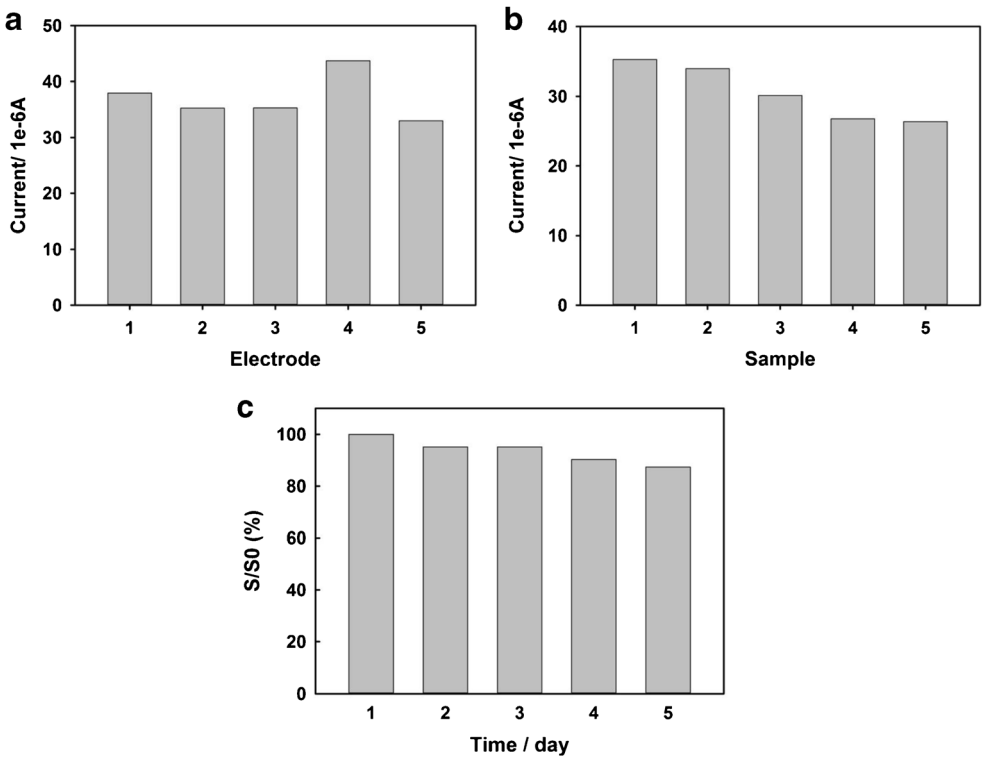

Fig. 6 (**a**) Reproducibility of five electrodes for detection of 4 mM glucose (**b**) Repeatability of one electrode for detecting 4 mM glucose for five times (**c**) Stability measurements of electrode for continuous five days

and electrolyte interface. Because of the exellent electrochemical performance, this non-enzymatic glucose sensor has great potential for continuous glucose monitoring in different areas such as biopharmacuetical industry and clinical usage.

Acknowledgments This work was supported by National Science Foundation (CBET-1805514) to HSZ.

References

1. Heller A, Feldman B (2008) Electrochemical glucose sensors and their applications in diabetes management. Chem Rev 108:2482–2505
2. Butler M (2005) Animal cell cultures: recent achievements and perspectives in the production of biopharmaceuticals. Appl Microbiol Biotechnol 68:283–291. https://doi.org/10.1007/s00253-005-1980-8
3. Butler M, Meneses-Acosta A (2012) Recent advances in technology supporting biopharmaceutical production from mammalian cells. Appl Microbiol Biotechnol 96:885–894. https://doi.org/10.1007/s00253-012-4451-z
4. Adley C (2014) Past, present and future of sensors in food production. Foods 3:491–510. https://doi.org/10.3390/foods3030491
5. Hwang DW, Lee S, Seo M, Chung TD (2018) Recent advances in electrochemical non-enzymatic glucose sensors – a review. Anal Chim Acta 1033:1–34. https://doi.org/10.1016/j.aca.2018.05.051
6. Huang J, Zhu Y, Yang X, Chen W, Zhou Y, Li C (2015) Flexible 3D porous CuO nanowire arrays for enzymeless glucose sensing: in situ engineered versus ex situ piled. Nanoscale 7:559–569. https://doi.org/10.1039/c4nr05620e
7. Dhara K, Mahapatra DR (2018) Electrochemical nonenzymatic sensing of glucose using advanced nanomaterials. Microchim Acta 185(1):49
8. Zhang P, Sun D, Cho A, Weon S, Lee S, Lee J, Han JW, Kim DP, Choi W (2019) Modified carbon nitride nanozyme as bifunctional glucose oxidase-peroxidase for metal-free bioinspired cascade photocatalysis. Nat Commun 10:940. https://doi.org/10.1038/s41467-019-08731-y
9. Ahmadalinezhad A, Chatterjee S, Chen A (2013) Synthesis and electrochemical study of nanoporous palladium-cadmium networks for non-enzymatic glucose detection. Electrochim Acta 112:927–932. https://doi.org/10.1016/j.electacta.2013.05.143
10. Zhou X, Zheng X, Lv R, Kong D, Li Q (2013) Electrodeposition of platinum on poly (glutamic acid) modified glassy carbon electrode for non-enzymatic amperometric glucose detection. Electrochim Acta 107:164–169. https://doi.org/10.1016/j.electacta.2013.05.146
11. Chinnadayyala SR, Park I, Cho S (2018) Nonenzymatic determination of glucose at near neutral pH values based on the use of nafion and platinum black coated microneedle electrode array. Microchim Acta 185:250–258. https://doi.org/10.1007/s00604-018-2770-1
12. Zhong SL, Zhuang J, Yang DP, Tang D (2017) Eggshell membrane-templated synthesis of 3D hierarchical porous au networks for electrochemical nonenzymatic glucose sensor. Biosens Bioelectron 96:26–32. https://doi.org/10.1016/j.bios.2017.04.038
13. Pal N, Banerjee S, Bhaumik A (2018) A facile route for the syntheses of Ni (OH)2and NiO nanostructures as potential candidates for non-enzymatic glucose sensor. J Colloid Interface Sci 516:121–127. https://doi.org/10.1016/j.jcis.2018.01.027
14. Luo J, Jiang S, Zhang H, Jiang J, Liu X (2012) A novel non-enzymatic glucose sensor based on cu nanoparticle modified graphene sheets electrode. Anal Chim Acta 709:47–53. https://doi.org/10.1016/j.aca.2011.10.025
15. Gao H, Xiao F, Ching CB, Duan H (2011) One-step electrochemical synthesis of PtNi nanoparticle-graphene nanocomposites for nonenzymatic amperometric glucose detection. ACS Appl Mater Interfaces 3:3049–3057. https://doi.org/10.1021/am200563f
16. Wang R, Liang X, Liu H, Cui L, Zhang X, Liu C (2018) Non-enzymatic electrochemical glucose sensor based on monodispersed stone-like PtNi alloy nanoparticles. Microchim Acta 185:339. https://doi.org/10.1007/s00604-018-2866-7
17. Ryu J, Kim K, Kim HS, Hahn HT, Lashmore D (2010) Intense pulsed light induced platinum-gold alloy formation on carbon nanotubes for non-enzymatic glucose detection. Biosens Bioelectron 26:602–607. https://doi.org/10.1016/j.bios.2010.07.021
18. Yang J, Jiang L, Zhang W, Gunasekaran S (2010) Talanta A highly sensitive non-enzymatic glucose sensor based on a simple two-step electrodeposition of cupric oxide (CuO) nanoparticles onto multi-walled carbon nanotube arrays. Talanta 82:25–33. https://doi.org/10.1016/j.talanta.2010.03.047
19. Long M, Tan L, Liu H, He Z, Tang A (2014) Novel helical TiO2nanotube arrays modified by Cu2O for enzyme-free glucose oxidation. Biosens Bioelectron 59:243–250. https://doi.org/10.1016/j.bios.2014.03.032
20. Liu L, Wang Z, Yang J, Liu G, Li J, Guo L, Chen S, Guo Q (2018) NiCo2O4 nanoneedle-decorated electrospun carbon nanofiber nanohybrids for sensitive non-enzymatic glucose sensors. Sensors Actuators B Chem 258:920–928. https://doi.org/10.1016/j.snb.2017.11.118
21. Batool R, Akhtar MA, Hayat A, Han D, Niu L, Ahmad MA, Nawaz MH (2019) A nanocomposite prepared from magnetite nanoparticles, polyaniline and carboxy-modified graphene oxide for non-enzymatic sensing of glucose. Microchim Acta 186:267. https://doi.org/10.1007/s00604-019-3364-2
22. Yu S, Peng X, Cao G, Zhou M, Qiao L, Yao J, He H (2012) Electrochimica Acta Ni nanoparticles decorated titania nanotube arrays as efficient nonenzymatic glucose sensor. Electrochim Acta 76:512–517. https://doi.org/10.1016/j.electacta.2012.05.079
23. Li X, Yao J, Liu F, He H, Zhou M, Mao N, Xiao P, Zhang Y (2013) Sensors and actuators B : chemical nickel / copper nanoparticles modified TiO 2 nanotubes for non-enzymatic glucose biosensors. Sensors Actuators B Chem 181:501–508. https://doi.org/10.1016/j.snb.2013.02.035
24. Guo YG, Hu JS, Wan LJ (2008) Nanostructured materials for electrochemical energy conversion and storage devices. Adv Mater 20:2877–2887. https://doi.org/10.1002/adma.200890061
25. Xiang JY, Wang XL, Xia XH, Zhang L, Zhou Y, Shi SJ, Tu JP (2010) Enhanced high rate properties of ordered porous Cu2O film as anode for lithium ion batteries. Electrochim Acta 55:4921–4925. https://doi.org/10.1016/j.electacta.2010.03.091
26. Berry BN, Dobrowsky TM, Timson RC, Kshirsagar R, Ryll T, Wiltberger K (2016) Quick generation of Raman spectroscopy based in-process glucose control to influence biopharmaceutical protein product quality during mammalian cell culture. Biotechnol Prog 32:224–234. https://doi.org/10.1002/btpr.2205
27. Zhu H, Li L, Zhou W, Shao Z, Chen X (2016) Advances in non-enzymatic glucose sensors based on metal oxides. J Mater Chem B 4:7333–7349. https://doi.org/10.1039/C6TB02037B
28. Liu M, Liu R, Chen W (2013) Graphene wrapped Cu2O nanocubes: non-enzymatic electrochemical sensors for the detection of glucose and hydrogen peroxide with enhanced stability. Biosens Bioelectron 45:206–212. https://doi.org/10.1016/j.bios.2013.02.010
29. Zhuang Z, Su X, Yuan H, Sun Q, Xiao D, Choi MMF (2008) An improved sensitivity non-enzymatic glucose sensor based on a CuO nanowire modified cu electrode. Analyst 133:126–132. https://doi.org/10.1039/b712970j
30. Jiang LC, De Zhang W (2010) A highly sensitive nonenzymatic glucose sensor based on CuO nanoparticles-modified carbon

nanotube electrode. Biosens Bioelectron 25:1402–1407. https://doi.org/10.1016/j.bios.2009.10.038

31. Yang Q, Long M, Tan L, Zhang Y, Ouyang J, Liu P, Tang A (2015) Helical TiO<inf>2</inf> nanotube arrays modified by Cu-Cu<inf>2</inf>O with ultrahigh sensitivity for the nonenzymatic electro-oxidation of glucose. ACS Appl Mater Interfaces 7:12719–12730. https://doi.org/10.1021/acsami.5b03401
32. Wang J, De Zhang W (2011) Fabrication of CuO nanoplatelets for highly sensitive enzyme-free determination of glucose. Electrochim Acta 56:7510–7516. https://doi.org/10.1016/j.electacta.2011.06.102
33. Wei H, Sun JJ, Guo L, Li X, Chen GN (2009) Highly enhanced electrocatalytic oxidation of glucose and shikimic acid at a disposable electrically heated oxide covered copper electrode. Chem Commun 2842–2844 . https://doi.org/10.1039/b904673a
34. Zhou Y, Ni X, Ren Z, Ma J, Xu J, Chen X (2017) A flower-like NiO-SnO2nanocomposite and its non-enzymatic catalysis of glucose. RSC Adv 7:45177–45184. https://doi.org/10.1039/c7ra07582k
35. Ahmad R, Vaseem M, Tripathy N, Hahn YB (2013) Wide linear-range detecting nonenzymatic glucose biosensor based on CuO nanoparticles inkjet-printed on electrodes. Anal Chem 85:10448–10454. https://doi.org/10.1021/ac402925r
36. Zhang X, Wang G, Liu X, Wu J, Li M, Gu J, Liu H, Fang B (2008) Different CuO nanostructures: synthesis, characterization, and applications for glucose sensors. J Phys Chem C 112:16845–16849. https://doi.org/10.1021/jp806985k